Severe Plastic Deformation by Fast Forging to Easy Produce Hydride from Bulk Mg-Based Alloys

Daniel Fruchart, Nataliya Skryabina, Patricia de Rango, Marjan Fouladvind, Valery Aptukov

Materials Transactions, Vol. 64, No. 8 (2023) pp. 1886 to 1893
Special Issue on Superfunctional Nanomaterials by Severe Plastic Deformation

Severe Plastic Deformation by Fast Forging to Easy Produce Hydride from Bulk Mg-Based Alloys

Daniel Fruchart[1,2,*], Nataliya Skryabina[2], Patricia de Rango[1], Marjan Fouladvind[1] and Valery Aptukov[3]

[1]*Institut Néel, CNRS & UGA, 38042 Grenoble, France*
[2]*JOMI-LEMAN SA, 74890 Fessy, France*
[3]*Perm State University, Bukireva, 614068 Perm, Russia*

The study of metal forging over long period of time has made it possible to establish the major basic principles up to the most recent, those of Severe Plastic Deformation (SPD). Thus the fundamental characteristics resulting from the stresses and deformations applied have led to the definition and modelling of microstructural variations in grain size and shape, density of dislocations, slip bands and twins, all factors to be considered during the transformation of the micro/nanostructure by SPD. For this purpose, SPD techniques such as ECAP, HPT, ARB have produced invaluable results namely in views of solid state hydrogen storage. So the present report focuses on magnesium-based materials with the aim of generating a deformed structure that will react quickly to allow massive and reversible hydrogen storage. However, all here above mentioned methods are rather difficult to scale up to mass production because they are either too time-consuming or too energy and labor intensive. Furthermore, it is revealed that at extreme, fast forging (FF) can introduce high densities of vacancies, voids and finally cracks in addition to grain refinement down to the ultrafine and nano-scale sizes. This leads in the FF worked material exhibiting excellent hydrogen reactivity as shown on a few examples. [doi:10.2320/matertrans.MT-MF2022049]

(Received March 23, 2023; Accepted May 24, 2023; Published July 25, 2023)

Keywords: *severe plastic deformation, fast forging, magnesium hydride, reaction kinetics*

1. Introduction

The highest performances of H-storage Mg-based materials have been revealed advantageous after forming the host metal by using both ways: 1 - Different Severe Plastic Deformation (SPD) methods such as HEBM,[1–6] HPT,[7–13] ECAP,[8–10,14–19] Intensive Rolling[20–22]... all leading to reduce the particles/crystallites to micro/nanometer sizes, 2 - Various additives said catalysts to boost hydrogen sorption.[22–26]

Mass production of MgH_2 must satisfy certain requirements with regard to processing conditions (ease, efficiency, cost etc.) and material performance (maximum hydrogen uptake, fast sorption, stability, reversibility, long lifetime) as reported in Ref. 27). This review aims to demonstrate that these can be achieved using Fast-Forging, a new and less conventional SPD method.[28–30] A large specific surface area is required in Mg-based materials for rapid hydrogen sorption as it is for all metals and alloys forming hydrides with a large and reversible storage capacity. However, with magnesium, additional criteria have to be considered since the change from metal to ionic-covalent bonding results in an extremely low bulk H-diffusion coefficient, $10^{-20}\,m^2\,s^{-1}$ at 305 K.[31] Clearly surface conditioning (see 2 above) is insufficient for the required objectives, and a high density of defects such as dislocations, slip bands, twins, grain boundaries, voids, vacancies and cracks is necessary for the improvement of bulk hydrogen transport.

Metal forging, a human activity going back to antiquity has progressively provided many ways to modify and optimize the microstructure of numerous metallic materials. In this paper we examine the potential for large scale operations via fast forging (FF) of magnesium alloys for the purpose of optimizing their hydrogen storage properties.

*Corresponding author: daniel.fruchart@neel.cnrs.fr

Forging is the oldest metalworking process,[32] and with the famous Damascus swords dating back to before 1000 CE, was combined with annealing. Carbon based nanostructures have recently been observed in these steels.[33] Now the wide range of forging modes as listed in the Refs. 34, 35) is related to the stress/strain diagram shown schematically in Fig. 1. The redistribution, modification and establishment of microstructural defects in the SPD regime (grain boundaries, dislocations, slip bands, twins and cracks) depend on forging kinetics, alloying elements and of course the resulting/peak temperature of the sample. Accordingly we aim to demonstrate the potential for large scale operation of Fast Forging (FF) on Mg-based materials to enhance the H-storage capacity. Practical FF consists of reducing by a factor of ten the height of ingots (bulk Mg, alloy or compacted composite) in $\sim 5 \times 10^{-3}$ secs. The initial temperature of the material can be achieved by induction heating. Since the mechanical energy of the hammer is almost fully dissipated in the material without plastic rebound it leads to a refinement of the grain size plastically and simultaneously overheats the

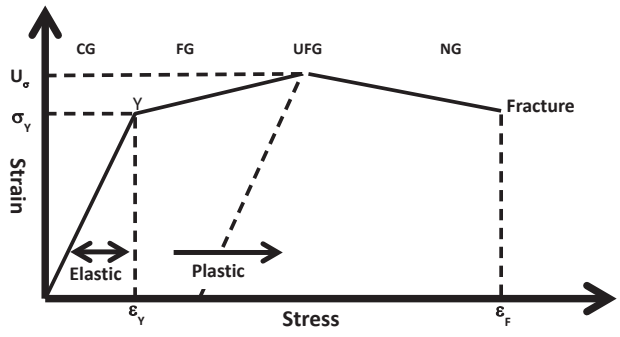

Fig. 1 Elastic-Plastic Stress-Strain scheme, ε_Y and ε_F for the stress yield and stress fracture respectively, σ_Y and U_σ for the strain yield and ultra-strain limit, respectively, CG, FG, UFG and NG indicating the coarse, fine, ultra-fine and nano-grain ranges.

material due to intense friction in between the particles.[28–30] In one FF pass, a very severe quasi-rolling is achieved and the crack (fracture) appearance threshold is reached.

Forging may be the oldest metalworking process in the world,[32] but with today's modern technology and process refinements, it offers renewed benefits. Over the years, the huge amounts of studies devoted to the Mg–MgH_2 transformation have led to the conclusion that fast kinetics and large H-uptake are necessary to achieve micro particles and nano-crystallites. It is well known that MgH_2 nucleation occurs at the free surfaces of crystallites and along grain boundaries. Because the diffusion coefficient of hydrogen in MgH_2 is very low, the classical process of interstitial jumps involved for most intermetallic hydrides is not pertinent. As reported in many review papers, a high density of defects, significant texture, specific additives as catalysts and interface elements are the most significant contributors to the enhancement of the hydrogen uptake process.[36] For a long period of time High Energy Ball Milling (HEBM) was the preferred technique for generating nanostructures and high defect density. Excellent results from other SPD techniques were reported more recently.[37] However, all these methods are difficult to scale up to mass production level due to energy cost or time and manpower limitations. Forging however can deliver a high density of voids, cracks and vacancies without those drawbacks.

2. On Magnesium Forging Conditions

Magnesium alloys are rather difficult to forge due to their low plasticity, low strain rate sensitivity and narrow forming temperature. Magnesium alloy forging to develop high mechanical strength characteristics is carried out between 300° and 450°C.[38] Using a semi-open die with a three-slide hot forging press (TSFP) is a new method applied to, for example, the AZ31 alloy (3.0 Al, $<$1.0 Zn w%) used in the aircraft industry.[39,40] This leads to improved tensile properties despite the lack of homogeneous grain size.[41] Even if applications of Mg alloys increase, e.g. for mobility purposes, forging of magnesium alloys with special dies remains expensive for engineering market uses. Casting is by far the preferred manufacturing method.

However, to deliver highly hydrogen active magnesium based materials, a versatile forging device has to be designed specifically, with a large range of functions that will be easy to modify on demand. Applied load, impact energy, die shape, temperature monitoring, are some of the parameters governing the microstructural characteristics obtained, as described above. The load should be adapted to the stiffness of the samples, in this case Mg, Mg alloys AZ31, AZ91 (8.5–9.0 Al, 0.45–0.9 Zn w%), ZK60 ($\sim$5.5 Zn, 0.45 Zr w%), Mg alloys (Ni Zn etc.), and Mg composites (extrusion compacted). Accordingly, both the values of the load and the kinetic energy at impact will determine the reduction factor of the sample, the effective deformation at grain scale, and the extent of void and crack formation. Die shape will also have an influence on these parameters. Open die forging then appears of interest in order to achieve fast flow to homogeneously radial-deform the material, and additionally to create a uniform texture. Indeed, all these characteristics can be well controlled if the temperature within the sample is *homogeneously* monitored. To achieve this, it is necessary to know the specific characteristics of the material:

a. The ductile-brittle transition temperature

b. The recrystallization temperature – this impacts on the formation of equiaxed grains, and also on the extent of grain growth prior to cooling.

c. The melting temperature of the different elements, if any, and potentially existing eutectic compositions.

From a number of reports on forging used to process metals and alloys able to absorb hydrogen, it is worth noting that an axisymmetric mode of deformation leads to homogeneous micro-structuration in the sample. Extrinsic parameters must be carefully considered in order to control the deformation process in terms of friction effects. Friction of the specimen between the plug and die may be reduced using a solid lubricant (graphite, BN). The dependence of internal friction of the grains within the sample on operating parameters (load, kinetic energy etc.) must be evaluated. These strong frictional effects can markedly affect the temperature of the material,[42–46] and therefore contribute to the final microstructural state. Finally a controlled neutral atmosphere around the processed sample is recommended.

3. Examples of Forging Hydrogen Absorbing Materials

A few examples are presented here in order to illustrate various factors related to the different forging conditions used.

a. S. Li *et al.*[45] have considered high temperature deformation in compression in the range 573–723 K temperature range of AZ91 alloy with various strain rates from 0.001 up to 1 s^{-1}, achieving a height reduction up to 55%. The experimental conditions here do not equate to fast forging conditions with UFG production; however, it does show evidence of the dynamic recrystallization process resulting in the formation of compact grains with $\sim$1 micron size. No hydrogenation procedure was undertaken; however one may presume that the hydrogen reaction would be slow.

b. J. Lang *et al.*[21,46,47] have forged ZK60 alloy at room temperature from compacted powder under various loads (17–43 MPa). The die was a closed die type, the forging load a $\sim$25 kg falling mass with the resulting strain rate at impact ranging from 150 to 300 s^{-1}. However, almost no reduction in height was observed apart from that corresponding to a small additional densification of the sample. The shock was mostly elastic, probably leading to a slight refinement of the grain structure and the initiation of a texture. Unfortunately neither XRD nor SEM are helpful in elucidating the effects of structural impacts. Hydrogen kinetic traces were recorded evidencing interesting features as shown in Figs. 2. In each case the H-uptake exhibits a marked incubation period of up to 2 hours, then MgH_2 nucleates rapidly up to a saturation level of $\sim$6%H. This global behavior could be compared to the results obtained for ECAP-type A processing[18,19] performed on AZ31 samples. Irrespective of the temperature, the anisotropic type A passing mode also demonstrates an incubation rest time contrary to the ECAP-type B_C. Here, the load at impact leads to only tiny effects as shown in Fig. 2(a) because the material was not laminated at forging. The

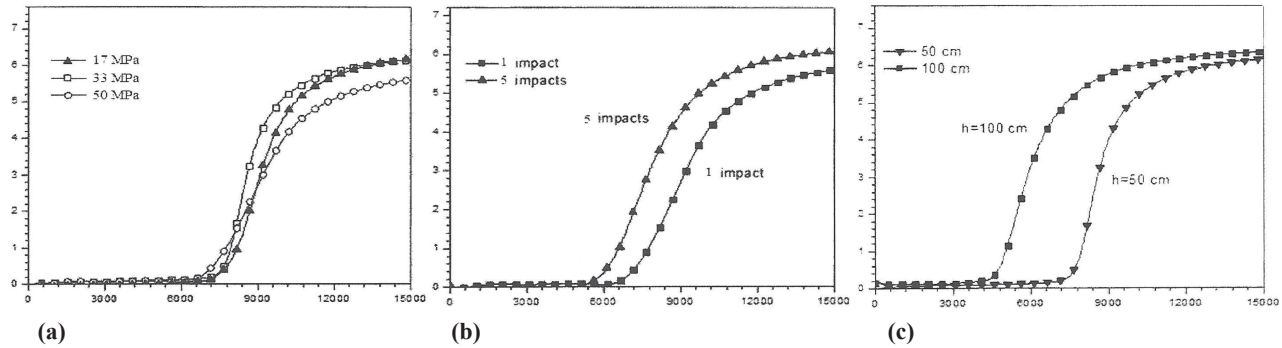

Fig. 2 Hydrogen absorption traces versus time (s) recorded under 2 MPa H_2 pressure at T = 350°C. (a) – under different loads with the same fastness, (b) – after 1, then two impacts with the same fastness, (c) – increasing the fastness for the same load.

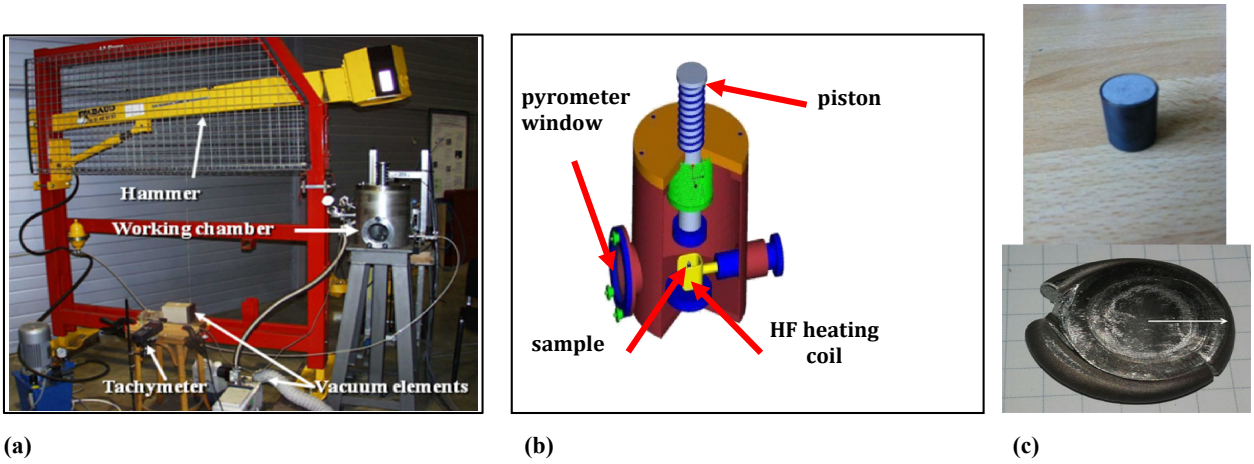

Fig. 3 Forging at Néel Institute, Grenoble. (a) – the machine with a hammer shocking the forging piston, equipped with a tachymeter and a fast camera, (b) – the chamber containing the sample that can be *in-situ* heated by a HF heating coil, (c) – up: the sample before forging and down; after forging.

incubation times shorten with increasing number of impacts as shown in Fig. 2(b); however the rate of loading appears to be the most important factor as shown in Fig. 2(c). Since here the apparent maximum hydrogen uptake for this alloy is $H_{max} = 7.1$ w% and it is evident that none of the samples were in a condition to absorb hydrogen quickly, similar to cast and non-mechanically-structured magnesium. The uptake was confirmed in a subsequent analysis where multi-CR and multi-CF reveal very similar hydrogenation properties.[47)]

c. Another type of forging operation made by O. Melilhova *et al.* is concerned with shock loading of Pd–H as pre-charged by the electrochemical route.[48)] In the hydrogenated state, Pd is harder than in the ductile annealed state. Positron lifetime spectroscopy was used as the appropriate experimental analysis technique, complemented by DFT calculations. High velocity forging of 6–8 × 10^3 s^{-1} leads to the development of high strain rates, and resulting temperature rises of up to ~200°C were noted. Two types of defects were induced during deformation, firstly a high density of dislocations, and secondly vacancy formation at crossing dislocations. Indeed Pd was the reference metal in experiments showing the formation of SAV, namely under several GPa hydrogen pressure.[49–51)] Interestingly this type of shock-loading experiment was followed by investigations by J. Gizek *et al.*[52)] They studied different types of compacted metals (FCC Ti and HCP Mg) by using the more conventional HPT process.[52)] Both dislocations and vacancies form efficient trap centers, this being relevant to the many developments devoted to the formation of MgH_2 nuclei in Mg using the conventional SPD ball-milling technique. To conclude the high strain developing approach, it is worth underlining that non-unique VAC states were created, but also large multi-vacancy clusters can be developed due to a reinforced stability. Experiments to show this were conducted on H-charged samples at H/Pd = 0.0, 0.0025, 0.075 and 0.25. As shown in Figs. 3(a), (b),[46)] it was found that both the densities of dislocations and VAC increase under the FF process versus the hydrogen content, the former being directly related to the square root of the hardness after shock loading.

d. Returning to Mg-rich compounds, S. E. Harandi *et al.*[53)] have used a stamping machine to test a sample of Mg–1%Ca using 110 tons force, a forging speed of 40 to 50 shocks per minute in an open die, the alloy heated successively to 250, 350, 450°C. The deformation rate was 34 ± 1%, and microhardness (45 ± 2 VPN) showed a small decrease when forging above 350° that can be attributed to grain refining by recrystallization. At first the study was oriented towards the biodegradable characteristics of the mechanically treated alloy. In fact more precipitation of Mg_2Ca, Figs. 2–4 of Ref. 53) at grain boundaries upon increasing the forging temperature made the alloy less suitable in terms of corrosion rate.

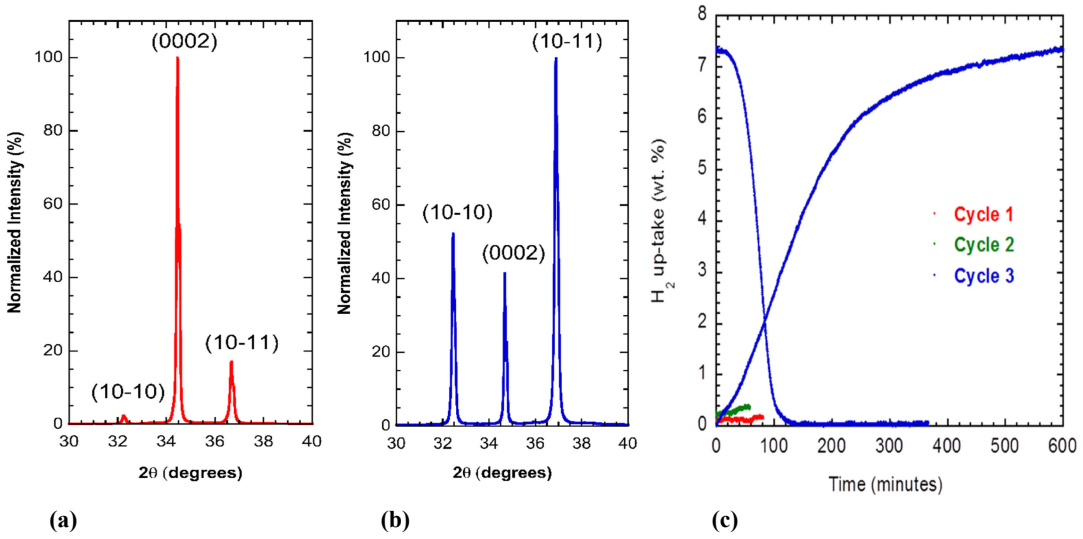

Fig. 4 XRD texture analysis, (a) – radial surface, (b) – along axis surface, and (c) - traces of hydrogen absorption (2 MPa)/desorption (150 kPa) under H_2 pressure after two activation cycles.

4. A Dedicated Forging Equipment

A specialized forging system for research purposes on magnets built earlier, and details can be found in previous reports.[28,54–59] Figure 4 shows a picture of this research scale forging system. One objective is to directly crystallize pseudo-ternary phases that would not normally form during conventional casting as evidenced by the equilibrium phase diagrams. The second objective is to promote refinement and texture of the grains before a final hydrogen decrepitation. The forging operation was carried out at ~850–1050°C in the ductile-brittle range and as a result of overheating during shock loading due to internal friction in the sample, fine grain recrystallization occurred together with the development of axial texture. The overheating upon shock loading was not exactly quantified, but was estimated to approach the melting point. The initial purpose was to deliver powders with fine enough microstructure for R–Fe–B hard magnet development where high coercive and anisotropic characteristics require ultra-fine crystallites in fine-grain material.[54,55]

Applied to the R–$Fe_{1-x}M_x$ (R = 4f, M = 3d elements) series of hard magnetic compounds, the shock load overheating allows the pseudo-ternary compound to fully form, as shown in Fig. 5. Interestingly, these types of compounds react rapidly with hydrogen, opening the routed of Hydrogen Decrepitation, HD,[54] and Hydrogen Disproportionation Dehydrogenation Recrystallization, HDDR,[56,57] both processes used in hard magnet technology. Furthermore, such experiments open perspectives to better design of the microstructure of powerful hydrogen absorbers such as Mg based alloys for reversible and large scale H-storage purposes.

5. Forging Mg-Based Materials for Hydrogen Storage

As reported elsewhere, these are the detailed processing conditions of various Mg-based materials submitted to fast forging with a view to enhancing the hydrogen reversible storage characteristics.[58,59] Mg compacts were prepared from

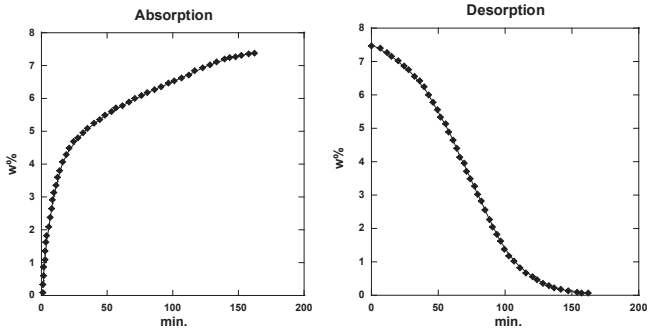

Fig. 5 First sorption rates of a (95 w% Mg + 5 w% MgH_2) compact directly after processed by Fast Forging. Left – at 320°C under 1 MPa H_2 pressure, Right – at 320°C under 15 kPa pressure.

Mg powder granules (40–80 μm) or preferably from atomized spherical (5–10 μm) particles provided by SFM SA[60] after pressing in a die at 1 ton/cm^2 pressure.[61] The sample submitted to forging was in the form of a cylinder (~20 mm height, 12–13 mm diameter) as shown Fig. 3(c)-top, introduced in a thin wall stainless steel tube. After one forging pass at RT, a sample prepared from SFM powder was in the form of a plate (~20 mm diameter, Fig. 3(c) bottom). Figures 4(a), (b) show the XRD pictures demonstrating a significant texture development, and Fig. 4(c) the kinetics of hydrogen uptake at 360°C under hydrogen pressure, (the sample has exhibited slow kinetics from 310 to 340°C, presumably the nucleation initiation stage). The mean crystallite size was estimated at 190 nm and a 14% strain rate was found from a Williamson-Hall analysis of XRD patterns.[61] The stability of MgH_2 upon SPD was discussed in Ref. 62).

Another batch of SFM powder was mixed with 5% MgH_2 prepared elsewhere then compacted in the same condition as above.[63] An attempt was made to compare the outcome with the previous test, acknowledging that the interface between Mg and MgH_2 favors the H/D reaction. Figures 5(left), (right) show that absorption/desorption corresponding to a H-uptake of 7 w% was achieved in 140 min. at 320°C under

1 MPa hydrogen pressure. With Mg only, this was H/Mg < or = 3 w% at 340°C under 2 MPa H_2.

It is worth noting that the same type of composite batches was also processed under the same conditions by two other SPD techniques, ECAP and CR.[63] A fast response was obtained using ECAP resulting in a 7% absorption in ~70 min under 1 MPa H_2 pressure at 320°C, but for CR5X (5 passes) the delay was much longer, giving ~7 w% absorption in >900 min. The experiments demonstrate the need for marked friction effects between the different phases in the material to create reacting surfaces. Without this effect, the results are only comparable with those using SPD routes and the more conventional magnesium alloys.[64]

Mechanical alloying in Mg–Ni mixtures by fast forging were reported earlier in several papers.[65–68] Experimentally this consisted in fast forging fine powders of Mg (5–10 µm from SFM, Ref. 60) and Ni (40–50 µm from Neyco-France, Ref. 69), mixed in proportion close to the hypo-eutectic composition, 78% Mg 22% Ni. In fact these types of combination have been tested elsewhere as mixtures and alloys using different SPD methods such as BM, ECAP and HPT[70–76] with the anticipation of finding better Mg–Ni materials for reversible hydrogen storage.

In a FF modelling approach, the compacted alloys considered were heated at various temperatures from RT up to ~550°C and then immediately forged. By numerical simulation the strain intensity fields developed under stress in the composite were imaged according to the size and stiffness of the components at the given temperatures.[67] The local deformation rate was established parallel to the compression strain axis in the sample as shown in Figs. 6(left), (right). The temperature increment was derived from the extent of material deformation, taking into account the particle size dependence of the friction effects. It was anticipated that the internal sample temperature should increase by ~200°C due to the conversion of the mechanical energy into heat. The temperature rise at low temperatures was also predicted to be greater than at high temperatures due to the contribution of ductile-brittle transition effects. Subsequent XRD and SEM investigations have revealed that in the high temperature range at least three phases can be observed, those being the initial Mg and Ni particles that are severely curried and larger Mg_2Ni grains at the base of the sample. Figure 7(left) illustrates the rate of synthesis of the binary Mg_2Ni versus the monitored temperature of the forging process.[65] Figure 7(right) shows the measured microhardness profile along the diameter of the forged plate at 420°C, indicating fairly homogeneous values. The synthesis temperature of Mg_2Ni agrees well with that revealed by SEM and XRD patterns recorded on the successively overheated samples.

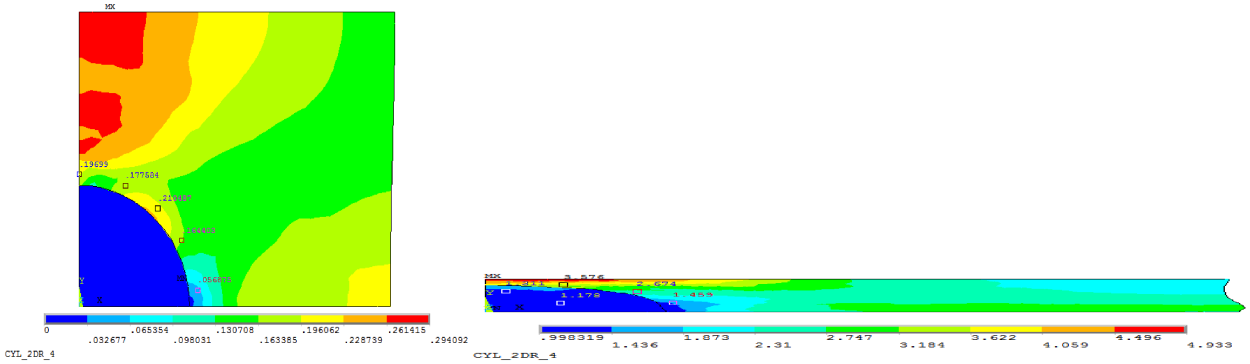

Fig. 6 Black is a low deformable Ni particle, the Mg main matter is progressively stressed (little grey = min. to dark grey = max.). Left – up to 10% and Down – up to 90% axial compression strain.

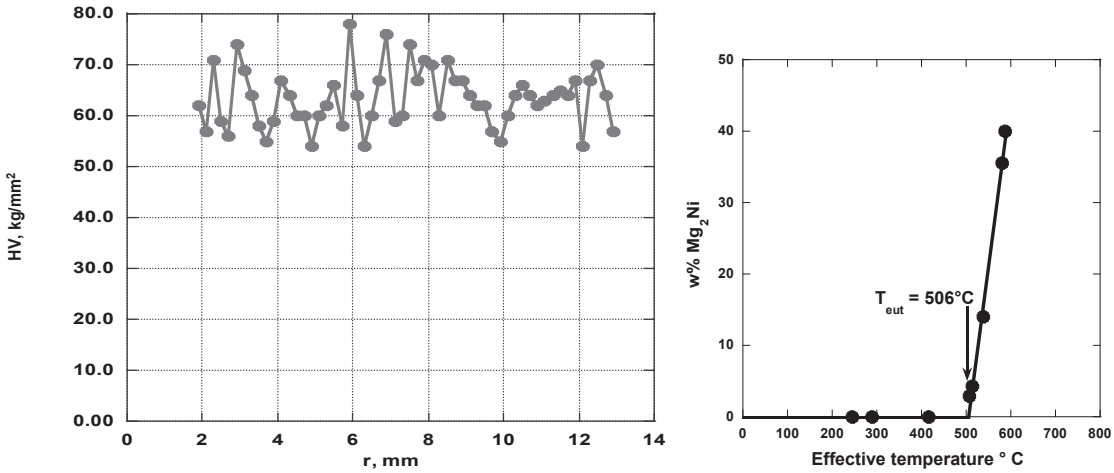

Fig. 7 Left - Micro-hardness measurement profile along the diameter of a forged plate (as shown Fig. 3(c)) at 420°C demonstrating fairly homogeneous HV values.[61] Right- Conversion rate of a ~Mg_{89}/Ni_{11} mixture to Mg_2Ni leading to some unreacted Mg and Ni, depending on the applied effective temperature. The mean overheating was estimated up to ~200°C, so that Mg_2Ni starts to form immediately above the eutectic temperature.[65]

Since samples forged at the lowest temperature have exhibited further, a greater reactivity to hydrogen than those forged at high temperature, the effective impact of formed Mg_2Ni should be questioned as being a catalyst. Conversely, cracks were observed when forging was carried out at the lowest temperatures owing to the less ductility. So, building a mechanical model allowing quantifies the forces exerted at the interfaces, the energy conditions to form MgH_2 nuclei within, or at surface of the Mg particles were questioned in Ref. 77). These investigations will not only concern with the SPD elaborated multiphase systems (Mg, MgH_2, Ni…), but as well operations operated under stress are accounted for. So the shear to stress field relationship indicates the preferable formation of elongated nuclei and supports the cracks development, benefit made for easier hydrogenation process.

In more recent experimental work, J. Wen *et al.*[78] have compared the structural properties and hydrogen reactivity of samples subject to three forging conditions: cold forging at RT (CF), hot forging at 450°C (HF) and annealing at 530°C prior to RT forging (A + CF). Detailed structural analyses (XRD, SEM, SEM-EBSD, texture) have confirmed the main characteristics as revealed before.[54,55,62] The average values of grain size are reported in Table 1.

Table 1 Average size of the grains (μm) versus the processing of the samples.

Sample	Mg	Mg_2Ni
CF	3.1 (0.2)	no
HF	2.7 (0.1)	3.7 (0.1)
ACF	4.5 (1.0)	2.6 (0.1)

Although the values are not very different, it should be noted that annealing the CF sample caused an increase in size of the Mg grains (with a large distribution), provoking the emergence of Mg_2Ni particles (at the expense of Ni grains) which then appear much smaller than those in the HF sample. It can be assumed that deformation and voids created at grain boundaries might play a role in the hydrogen diffusion process. Interestingly, it was emphasized that for the first CF and A + CF samples, the H-absorption cycle exhibits the highest performance with ~6 w% (theoretical value 5.92 w%) compared with the conventional SPD techniques.[41,43] Furthermore, as shown in Figs. 8, after application of a sufficient number of H/D cycles, (~10), all the forged samples exhibit the same fast initial absorption kinetics and equal saturation levels (~4.2 w% H) expected due to the similar microstructures. This equal saturation levels demon-

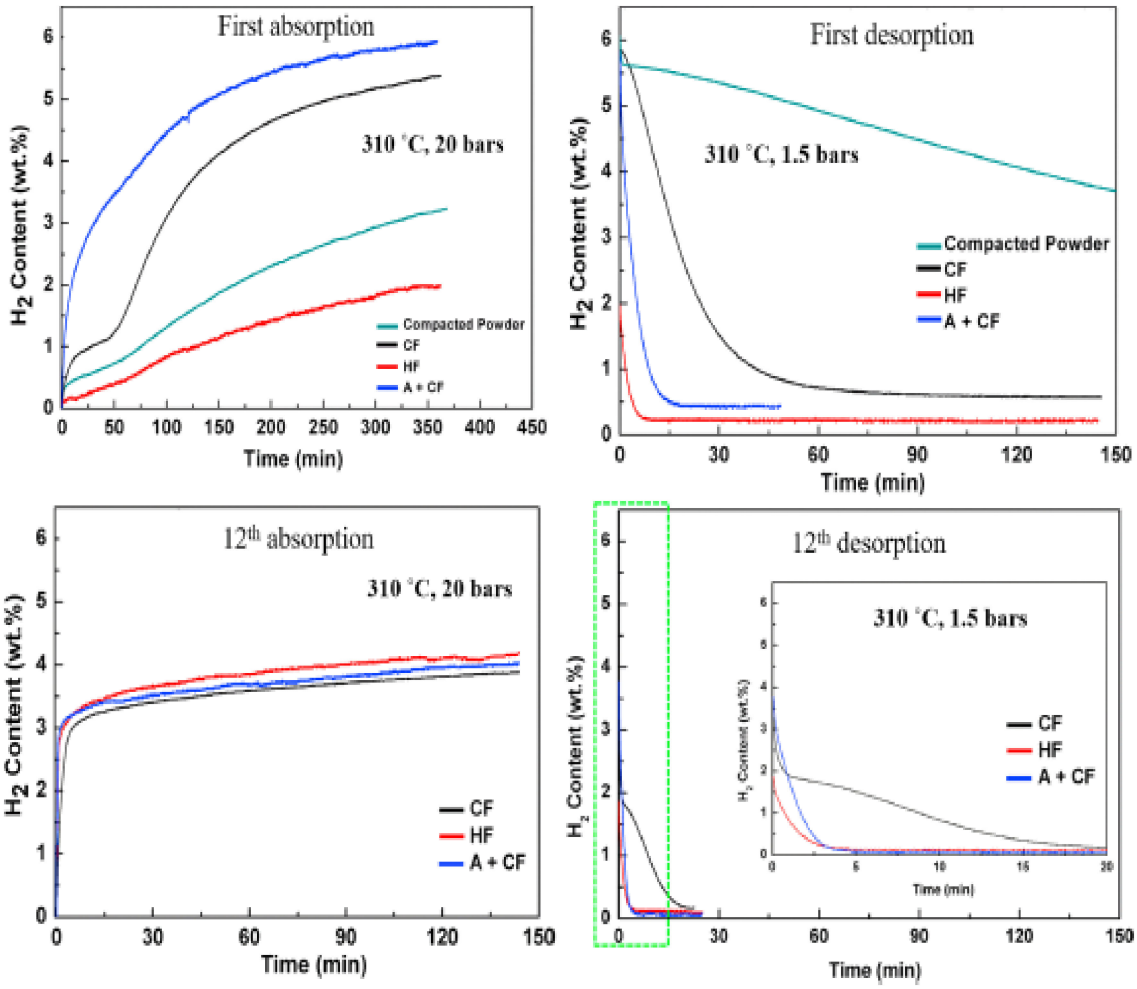

Fig. 8 Up left and right – 1st absorption and desorption traces respectively, for initial compact, CF, HF and A + CF materials. Down left and right – 12th absorption and desorption traces respectively, for CF, HF and A + CF materials.

strate that after the different forging vs. hydrogenation treatments (CF + H-cycles, HF and finally ACF that that most of the nickel was combined with magnesium to form Mg_2Ni, subsequently hydrogenated. At desorption, evidence of the catalytic positive role of the less stable ternary hydride Mg_2NiH_{4-x} was anticipated to easy the desorption process.

Finally, J. Wen *et al.*[79] have conducted *in-situ* neutron scattering experiments under deuterium (hydrogen) atmosphere on room temperature fast forged Mg–Ni powder mixture. These experiments demonstrate the defect-containing fiber microstructure allows first uptake of deuterium. This occurs at temperatures as low as 250°C (so ~100°C lower than the formation of MgD_2) although no evidence of the presence of Mg_2Ni-type nuclei was detected. In fact such Mg–Ni-based systems form at temperatures immediately above. Then, upon heating further, concomitant reactions between $Mg_2NiD_{0.3}$, Mg_2NiD_4 and Mg lead to the fast formation of MgD_2 in a catalytic-type process. The solid solution system was recognized as the facilitating phase at the interface for rapid growth of MgD_2 particles, both during the absorption and desorption reactions. Since the $MgNi_2D_4$ is fully destabilized above 250°C, this corroborated the partial amount of a unique and stable MgD_2 formed at 310°C under 2 MPa gas pressure as shown Fig. 8 (down-left).

6. Conclusion

Forging metals and alloys known to facilitate the reversible absorption of significant amounts of hydrogen – more particularly in the Mg-based series, and is of high interest as an effective competitor to the conventionally used SPD techniques such as HEBM, ECAP, HPT, CRX, ARB. A major advantage of forging is flexibility of the process, in that it can be adapted to a variety of service requirements. In particular the impact velocity and peak load can be readily controlled. Specific designs of the anvil and die modify the pattern of plastic flow in the sample, and hence allow the development of desired microstructure. The transient heat created in the sample by the transformation of mechanical energy is a contributing factor to the development and modification of microstructure and texture. These structural transformations are uniform throughout the volume of the sample.

Fast forging enables rapid processing and is easy to automate, and mass production machines should be developed in the near future.

Acknowledgement

The authors warmly thank DR. Charles May (MCD in the School of Engineering at the University of Greenwich) for a critical reading of the manuscript.

REFERENCES

1) B. Vigeholm, J. Kjøller, B. Larsen and A.S. Pedersen: J. Less-Common Met. **89** (1983) 135–144.
2) E. Ivanov, I. Konstanchuk, A. Stepanov and V. Boldyrev: J. Less-Common Met. **131** (1987) 25–29.
3) Y. Chen and J.S. Williams: J. Alloy. Compd. **217** (1995) 181.
4) R. Schulz, S. Boily, L. Zaluski, A. Zaluska, P. Tessier and J.O. Ström-Olsen: Nanocrystalline Materials for Hydrogen Storage, Innovations in Metallic Materials (1995) pp. 529–535.
5) L. Zaluski, A. Zaluska and J.O. Ström-Olsen: J. Alloy. Compd. **253–254** (1997) 70–79.
6) R.A. Dunlap, Z.H. Cheng, G.R. MacKay, J.W. O'Brien and D.A. Small: Hyperfine Interact. **130** (2000) 109–126.
7) A. Yamashita, Z. Horita and T.G. Langdon: Mater. Sci. Eng. A **300** (2001) 142–147.
8) D.R. Leiva, D. Fruchart, M. Bacia, G. Girard, N. Skryabina, A.C.S. Villela, S. Miraglia, D.S. Santos and W.J. Botta: Int. J. Mat. Res. (formerly Z. Metallk.) **100** (2009) 1739–1746.
9) D.R. Leiva, A. Moreira Jorge, T.T. Ishikawa, J. Huot, D. Fruchart, S. Miraglia, C.S. Kiminami and W.J. Botta: Adv. Eng. Mater. **12** (2010) 786–792.
10) J. Huot, N.Y. Skryabina and D. Fruchart: Metals **2** (2012) 329–343.
11) K. Edalati, K. Kitabayashi, Y. Ikeda, J. Matsuda, H.-W. Li, I. Tanaka, E. Akiba and Z. Horita: Scr. Mater. **157** (2018) 54–57.
12) K. Kitabayashi, K. Edalati, H.-W. Li, E. Akiba and Z. Horita: Adv. Eng. Mater. **22** (2020) 1900027.
13) Á. Révész and M. Gajdics: Energies **14** (2021) 819.
14) G.S. Lima, D.R. Leiva, J. Huot, T. Ishikawa, C. Bolfarini and C.S. Kiminami: Mater. Sci. Forum **667–669** (2011) 1047–1052.
15) V.M. Skripnyuk, E. Rabkin, Y. Estrin and R. Lapovok: Acta Mater. **52** (2004) 405–414.
16) R.B. Figueiredo and T.G. Langdon: Mater. Sci. Eng. A **501** (2009) 105–114.
17) V.M. Skripnyuk, M. Rabkin, Y. Estrin and R. Lapovok: Int. J. Hydrogen Energ. **34** (2009) 6320–6324.
18) N.E. Skryabina, V.N. Aptukov, P.V. Romanov and D. Fruchart: PNRPU Mechanics Bulletin **1–2** (2018) 102–107.
19) N. Skryabina, V. Aptukov, P. Romanov, D. Fruchart, P. de Rango, G. Girard, C. Grandini, H. Sandim, J. Huot, J. Lang, R. Cantelli and F. Leardini: Molecules **24** (2019) 89.
20) R. Mori, H. Miyamura, S. Kikuchi, K. Tanaka, N. Takeichi, H. Tanaka, N. Kuriyama, T.T. Ueda and M. Tsukahara: Mater. Sci. Forum **561–565** (2007) 1609–1612.
21) J. Lang and J. Huot: J. Alloy. Compd. **509** (2011) L18–L22.
22) S.D. Vincent, J. Lang and J. Huot: J. Alloy. Compd. **512** (2012) 290–295.
23) J.L. Bobet, B. Chevalier and B. Darriet: J. Alloy. Compd. **330–332** (2002) 738–742.
24) S. Rivoirard, P. de Rango, D. Fruchart, J. Charbonnier and D. Vempaire: J. Alloy. Compd. **356–357** (2003) 622–625.
25) A. Zaluska and L. Zaluski: J. Alloy. Compd. **404–406** (2005) 706–711.
26) A.J. Du, S.C. Smith, X.D. Yao, C.H. Sun, L. Li and G.Q. Lu: Appl. Phys. Lett. **92** (2008) 163106.
27) M. Jehan and D. Fruchart: J. Alloy. Compd. **580** (2013) S343–S348.
28) S. Rivoirard, D. Chateigner, P. de Rango, D. Fruchart, R. Perrier de la Bâthie and J.L. Soubeyroux: Philos. Mag. A **80** (2000) 1955–1966.
29) P. de Rango, D. Fruchart, V. Aptukov and N. Skryabina: Int. J. Hydrogen Energ. **45** (2020) 7912–7916.
30) J. Huot, S. Amira, J. Lang, N. Skryabina and D. Fruchart: IOP Conf. Ser. Mater. Sci. Eng. **63** (2014) 012114.
31) C. Zhou, Z. Jingxi, R. Bowman and Z.Z. Fang: Inorganics **9** (2021) 36.
32) https://en.wikipedia.org/wiki/Iron_Age.
33) K. Sanderson: Nature **444** (2006) 286. S2CID 136774602.
34) J.R. Davis: *Handbook: Forming and Forging: 14*, 9th ed., (ASM Intl, 1989) ISBN-10: 0871700204, ISBN-13: 978-0871700209 Metals.
35) K. Gissing: *The Book of Forging: Basic Techniques & Examples*, 1st ed., (Schiffer Craft, Pennsylvania, 2019), ISBN-10: 0764357379, ISBN-13: 978-0764357374.
36) V.A. Yartys *et al.*: Int. J. Hydrogen Energ. **44** (2019) 7809–7859.
37) K. Edalati, E. Akiba, W. Botta, Y. Estrin, R. Floriano, D. Fruchart, T. Grosdidier, Z. Horita, J. Huot, H.-W. Li, H.-J. Lin, A. Revesz and M. Zehetbauer: J. Mater. Sci. Technol. **146** (2023) 221–239.
38) N.P. Papenberg, S. Gneiger, I. Weissensteiner, J. Grasserbauer, G. Falkinger, S. Pogstscher and F. Roters: Materials **13** (2020) 985.
39) A. Dziubińska, A. Gontarz, M. Dziubiński and M. Barszcz: Adv. Sci. Technol. Res. J. **10** (2016) 158–168.
40) A. Dziubinska and A. Gontarz: Aircraft Engineering & Aerospace

Techn. **87** (2015) 180–188.
41) A. Dziubińska, A. Gontarz, K. Horzelska and P. Pieśko: Procedia Manuf. **2** (2015) 337–341.
42) F. Kisuka, C.-Y. Wu and C. Hare: EPJ Web Conf. **249** (2021) 05007.
43) A. Gontarz, K. Drozdowski, J. Michalczyk, S. Wiewiórowska, Z. Pater, J. Tomczak, G. Samołyk, G. Winiarski and P. Surdacki: Materials **14** (2021) 32.
44) R. Matsumoto and K. Osakada: Mater. Trans. **45** (2004) 2838–2844.
45) S. Li, Y.-Q. Wang, M. Zheng and K. Wu: Trans. Nonferrous Met. Soc. China **14** (2004) 306–310. id:1003-6326(2004)02-0306-05
46) J. Lang: PhD Thesis, Univ. du Québec à Trois-Rivières, (2016) p. 121.
47) D.R. Leiva, R. Floriano, J. Huot, A.M. Jorge, C. Bolfarini, C.S. Kiminami, T.T. Ishikawa and W.J. Botta: J. Alloy. Compd. **509** (2011) S444–S448.
48) O. Melikhova, J. Cizek, Y. Chen, T. Suo, I. Prochazka and F. Liu: J. Alloy. Compd. **645** (2015) S472–S475.
49) Y. Fukai, H. Ishikawa, T. Goto, J. Susaki, T. Yagi, J.L. Soubeyroux and D. Fruchart: Zeits. Physik. Chemie NF **163** (1989) 479–482.
50) Y. Fukai: J. Alloy. Compd. **231** (1995) 35–40.
51) D.S. dos Santos, S. Miraglia and D. Fruchart: J. Alloy. Compd. **291** (1999) L1–L5.
52) J. Čížek, O. Melikhova, Z. Barnovská, I. Procházka and R.K. Islamgaliev: J. Phys.: Conf. Ser. **443** (2013) 012008.
53) S.E. Harandi, M.H. Idris and H. Jafari: Mater. Des. **32** (2011) 2596–2603.
54) S. Rivoirard: PhD thesis, Univ. J. Fourier Grenoble, (France, 1999) p. 284.
55) I. Popa, P. de Rango, D. Fruchart and S. Rivoirard: J. Magn. Magn. Mater. **242–245** (2002) 1388–1390.
56) S. Liesert, A Kirchner, W Grünberger, A. Handstein, P. de Rango, D. Fruchart, L. Schultz and K.H. Müller: J. Alloy. Compd. **266** (1998) 260–265.
57) D. Fruchart, P. de Rango, S. Miraglia and S. Rivoirard: J. Metastab. Nanocryst. Mater. **20–21** (2004) 725–738.
58) D. Fruchart and N. Skryabina: Proceedings GSAM2016, Promoting Functionnality by Severe Plastic Deformation: Significance of Lattice Defects and Phase Transformations, 1, (2016) p. 3.
59) J. Grbović Novaković, N. Novaković, S. Kurko, S. Milošević Govedarović, T. Pantić, B. Paskaš Mamula, K. Batalović, J. Radaković, J. Rmuš, M. Shelyapina, N. Skryabina, P. de Rango and D. Fruchart: ChemPhysChem **20** (2019) 1216–1247.
60) SFM SA, Société pour la Fabrication du Magnésium, Rue des Sablons 9, (Martigny, Switzerland, 1920) https://www.sfm-magnesium.ch.
61) P. de Rango, J. Wen, N. Skryabina, L. Laversenne, D. Fruchart and M. Borges: Energies **13** (2020) 3509.
62) N. Skryabina, N. Medvedeva, A. Gabov, D. Fruchart, S. Nachev and P. de Rango: J. Alloy. Compd. **645** (2015) S14–S17.
63) M. Fouladvind: IUP GSI-UJF MSc Report, Univ. J. Fourier, (Grenoble, France, 2010).
64) D.R. Leiva, A.M. Jorge, T.T. Ishikawa, J. Huot, D. Fruchart, S. Miraglia, C.S. Kiminami and W.J. Botta: Adv. Eng. Mater. **12** (2010) 786–792.
65) N. Skryabina, V.N. Aptukov, P. de Rango and D. Fruchart: Int. J. of Hydrogen Energ. **45** (2020) 3008–3015.
66) P. de Rango, D. Fruchart, V. Aptukov and N. Skryabina: Int. J. Hydrogen Energ. **45** (2020) 7912–7916.
67) V.N. Aptukov, N. Skryabina and D. Fruchart: PNRPU Mechanics Bulletin **2** (2020) 5–15.
68) V.N. Aptukov, I.I. Tsirulnik, N.E. Skryabina and D. Fruchart: PNRPU Mechanics Bulletin **3** (2021) 12–21.
69) Neyco-France: Chemical Manufacturing, 30, Avenue de la Paix, 92170 Vanves, France, https://www.neyco.fr.
70) A. Stepanov, E. Ivanov, I. Konstanchuk and V. Boldyrev: J. Less-Common Met. **131** (1987) 89–97.
71) L. Zaluski, A. Szuluska and J.O. Ström-Olsen: J. Alloy. Compd. **217** (1995) 245–249.
72) A. Zaluska, L. Zaluski and J.O. Ström-Olsen: J. Alloy. Compd. **289** (1999) 197–206.
73) P. Tessier and E. Akiba: J. Alloy. Compd. **293–295** (1999) 400–402.
74) V. Skripnyuk, E. Buchman, E. Rabkin, Y. Estrin, M. Popov and S. Jorgensen: J. Alloy. Compd. **436** (2007) 99–106.
75) S. Pedneault, J. Huot and L. Roué: J. Power Sources **185** (2008) 566–569.
76) T. Hongo, K. Edalati, M. Arita, J. Matsuda, E. Akiba and Z. Horita: Acta Mater. **92** (2015) 46–54.
77) V.N. Aptukov, N.E. Skryabina and D. Fruchart: PNRPU Mechanics Bulletin **2** (2022) 23–35.
78) J. Wen, P. de Rango, N. Allain, L. Laversenne and T. Grosdidier: J. of Power Sources **480** (2020) 228823.
79) J. Wen, L. Laversenne, M. Novelli, T. Grosdidier and P. de Rango: J. Alloy. Compd. **947** (2023) 169543.